ACADEMIC PRESS

Available online at www.sciencedirect.com

SCIENCE DIRECT®

Journal of Computational Physics 184 (2003) 649–669

JOURNAL OF COMPUTATIONAL PHYSICS

www.elsevier.com/locate/jcp

A stochastic approach for the numerical simulation of the general dynamics equation for aerosols

Edouard Debry[a], Bruno Sportisse[a,*], Benjamin Jourdain[b]

[a] *Centre d'enseignement et de Recherche sur l'Eau la Ville et l'Environnement, Ecole, Nationale des Ponts et Chaussées (ENPC-CEREVE), 6-8 Avenue Blaise Pascal, 77455 Champs sur Marne, France*

[b] *Centre d'Enseignement et de Recherche en Mathématiques, Informatique et Calcul Scientifique, Ecole Nationale des Ponts et Chaussées (ENPC-CERMICS), 6-8 Avenue Blaise Pascal, 77455 Champs sur Marne, France*

Received 19 March 2002; accepted 17 October 2002

Abstract

We present in this article a stochastic algorithm based mainly on [Monte Carlo Methods and Applications 5(1) (1999) 1; Stochastic particle approximations for Smoluchowski's coagulation equation. Technical Report, Weierstrass-Institut for Applied Analysis and Stochastics, 2000. Preprint No. 585] applied to the integration of the General Dynamics Equation (GDE) for aerosols . This algorithm is validated by comparison with analytical solutions of the coagulation–condensation model and may provide an accurate reference solution in cases for which no analytical solution is available.

AMS: 65C05; 86A10

Keywords: Air pollution modeling; Atmospheric aerosols; Coagulation; Condensation; Evaporation; Nucleation; Aerosol size density; General dynamics equation; Stochastic resolution; Size-resolved methods

1. Introduction

The gas-phase pollution has been widely investigated [3] and numerous three-dimensional models are available. The next step is now to take into account the atmospheric particulate matter. Aerosols may indeed have a strong impact on the atmospheric radiative balance, on the gas-phase concentrations (especially through the gas to particle conversion) and on man health.

Aerosol modeling in current 3D atmospheric Chemistry-Transport Models is usually made by appropriate parameterizations [4]. Size-resolved models are however a key issue [5] since many properties of aerosols are deeply related to the size. It is also important to follow the aerosol size distribution (or density),

* Corresponding author. Tel.: +33-1-6415-3577; fax: +33-1-6415-3764.
E-mail addresses: debry@cereve.enpc.fr (E. Debry), sportiss@cereve.enpc.fr (B. Sportisse), jourdain@cermics.enpc.fr (B. Jourdain).

0021-9991/02/$ - see front matter
PII: S0021-9991(02)00041-4

let us note ASD, along time. The ASD evolution is modelized by the General Dynamics Equation (GDE) [3] which takes into account the physical processes of aerosols as coagulation, condensation/evaporation, nucleation, and removal.

Some models already exist to solve this equation and we will distinguish the so-called *multi-modal models* for which an a priori form is chosen for the ASD and the *size-resolved models* which directly solve the GDE with appropriate numerical schemes.

In multi-modal model the ASD is usually assumed to be a sum of log-normal densities, and the GDE is solved through the ASD moments. We refer for instance to [6,7]. The advantage of this method is a few number of parameters and a rather easy implementation. The limitation is however a possible lack of accuracy since the only first moments of the ASD have been preserved.

In size-resolved methods the aerosol size spectrum is discretized into a finite number of bins and the GDE is solved within each bin, whatever the numerical scheme is. This kind of method can be performed in two different ways whether one solves each process separately or not.

Splitting is usually advocated in order to focus on each process separately. Coagulation is usually solved with "size binning" algorithms. We refer for instance to [8,9]. The drawbacks of this method are the lack of convergence results and the diffusion for large bins. Condensation/evaporation leads to an advection-equation for the ASD for which many algorithms have been developed [10].

Nevertheless splitting always introduces a "splitting error" and the aerosol size grid may be different for each process, which may imply some numerical difficulties.

With a *coupling* approach all physical processes are solved in the same time. This can be for instance performed by finite elements methods applied to the whole GDE [11–13].

However, the main drawbacks of the previous approaches are the lack of theoretical results proving the convergence of the numerical solution to the solution of the GDE. The GDE can be solved analytically for academic cases only and validation for such cases does not ensure a good behaviour in more realistic situations. The lack of reference solution has already been underlined for instance in [14]. Searching a numerical reference solution, not necessary for operational purposes, is therefore a key issue. Such reference solutions do not have necessary to be computationaly efficient but highly accurate in order to be used in benchmarks of fast numerical methods as those listed above.

Stochastic methods are good candidates for this role. They have already been used to solve the Boltzmann equation [15,16] and more recently to solve the coagulation equation [1,2,17]. The key advantage of these methods is that they rely on a stochastic formulation of the GDE, which provides a basis for their validity. They are moreover rather easy to implement.

We propose in this article an extension of such approaches to the whole GDE for single component aerosols. The article is organized as follows: in Section 2 we briefly summarize the key features for the GDE and we present the mass flow formulation. We present our algorithm in Section 3. Some numerical tests are summarized in Section 4.

2. General dynamics equation and mass flow formulation

Notations and dimensions. In the following article the letters v and r will, respectively, always represent the volume and the radius of one physical aerosol,[1] they are expressed, respectively, in μm^3 and μm. We will refer either to v of r as the "aerosol size." We assume one single aerosol is completely described by its size.

The term *particle* will constantly refer to *numerical particle*, which is defined in Section 2.2.

Air volumes are expressed in cm^3, the aerosol concentration in air is then expressed in #aerosols cm^{-3}. We assume the specific mass of aerosols to be size and time independent, then the aerosol volume and mass

[1] v and r are related by $v = \frac{4}{3}\pi r^3 \iff r = \left(\frac{3v}{4\pi}\right)^{\frac{1}{3}}$.

concentration are equivalent. In order to avoid confusion between volumes of different kinds, we will always talk about aerosol mass concentration although it is in fact the volume concentration expressed in $\mu m^3\ cm^{-3}$.

The ASD describes the repartition of aerosol concentrations with respect to their size. This one is usually represented by a continuous density of concentration $n(v,t)$ so that $n(v,t)\,dv$ is the concentration of aerosols whose sizes range between v and $v+dv$ at time t. Then the dimension of $n(v,t)$ is #aerosols $cm^{-3}\ \mu m^{-3}$. Let us note $q(v,t)$ the aerosol mass density, which is merely derived from n by $q(v,t)=vn(v,t)$.

The relative densities will be noticed $\tilde{n}$ and $\tilde{q}$.

2.1. General dynamics equation

For a single component aerosol, the time evolution of n is then given by the following equation [3]:

$$\frac{\partial n}{\partial t}(v,t) = \underbrace{\frac{1}{2}\int_{v_0}^{v-v_0} K(u,v-u)n(u,t)n(v-u,t)\,du}_{\text{coagulation gain}} - \underbrace{n(v,t)\int_{v_0}^{\infty} K(u,v)n(u,t)\,du}_{\text{coagulation loss}} - \underbrace{\frac{\partial(I_0 n)}{\partial v}(v,t)}_{\text{condensation}} + \underbrace{\delta_{(v_0,v)}J_0(t)}_{\text{nucleation}} - \underbrace{R(v,t)n(v,t)}_{\text{deposition}}, \tag{1}$$

where $K(u,v)$, $I_0(v,t)$, $J_0(t)$, and $R(v,t)$ are, respectively, the coagulation, condensation/evaporation, nucleation, and deposition kernels. The physical properties of each process is entirely described by their kernel expression. According to the previous notations $K(u,v)$ is in $cm^3\ s^{-1}$, $I_0(v,t)$ in $\mu m^3\ s^{-1}$, $J_0(t)$ in #aerosols $cm^{-3}\ s^{-1}$, and $R(v,t)$ in s^{-1}.

Aerosol size spectrum. The smallest size v_0 is the aerosol size from which and aerosol becomes stable and begins to grow, it is then the nucleation size. The coagulation loss term implies an infinite integral, actually as large aerosols are finally removed from atmosphere by gravitational settling, ∞ can be replaced by the maximum v_{max} of aerosol size existing in the atmosphere.

Atmospheric aerosols radius usually range from 0.001 to 100 μm, which makes the atmospheric aerosol Dynamics lie from the free molecular regime ($K_n \geqslant 10$)[2] to the continuous one ($K_n \leqslant 0.1$). Then expressions of various kernels have to take into account both regimes. The nucleation kernel is not concerned as this process does not influence already existing aerosols.

In Sections 2.1.1 and 2.1.2 we derive the usual expressions of the coagulation and condensation/evaporation kernels in the continuous regime, their complete expressions are given in Appendix A.

2.1.1. Coagulation kernel

The coagulation is mostly due to the Brownian activity [18], which may be written in the continuous regime for spheric aerosols of size u and v as

$$K(u,v) = \frac{2k_b T}{3\mu_{air}}\left[2 + \left(\frac{u}{v}\right)^{\frac{1}{3}} + \left(\frac{v}{u}\right)^{\frac{1}{3}}\right], \tag{2}$$

where $k_b = 1.381\times10^{-23}\ J\ K^{-1}$ is Boltzmann's constant, μ_{air} the dynamic viscosity of air, and T is the air temperature.

[2] K_n is the Knudsen number, ratio between the mean free path of air, λ_{air}, and the particle radius, for average atmospheric conditions $\lambda_{air} = 0.0651$ μm.

That is to note the Brownian kernel can be considered in first approximation as a constant, indeed for equal size aerosols the coagulation kernel is reduced to

$$K(u,u) = \frac{8k_b T}{3\mu_{air}}. \tag{3}$$

Therefore this constant is usually called the Brownian constant and is equal to 6.405×10^{-10} cm^3 s^{-1} for average atmospheric conditions.

2.1.2. Condensation/evaporation kernel

The condensation/evaporation process describes the relaxation to an equilibrium between aerosol and gas phases for one chemical species i. The equilibrium is usually achieved by a diffusion process between the bulk gas and the aerosol surface, the condensation kernel is then written for aerosol of size v in the continuous regime as [3]

$$I_0(v,t) = \frac{4\pi D_i M_i}{\rho_p RT}\left(\frac{3v}{4\pi}\right)^{\frac{1}{3}}(p_i^\infty - p_i^{eq}), \tag{4}$$

where D_i is diffusion coefficient of species i in air and M_i its molar weight, ρ_p the specific mass of aerosols, assumed to be independent of the particle size, and $R = 8.314$ J mol^{-1} K^{-1} is the molar gas constant.

The difference between the vapor pressure of i far from the particle, p_i^∞, and the equilibrium vapor pressure, p_i^{eq}, is the driving force for transport of i. The latter is the result from thermodynamic equilibrium between gas and aerosol phase, some models have been developed for multicomponents aerosols, as Isorropia [19]. There is effective condensation when $p_i^\infty \geqslant p_i^{eq}$ $(I_0(v,t) \geqslant 0)$ and effective evaporation when $p_i^\infty \leqslant p_i^{eq}$ $(I_0(v,t) \leqslant 0)$.

Eq. (4) can be rewritten as

$$I_0(v,t) = \sigma_i(t) v^{\frac{1}{3}}, \quad \sigma_i(t) = \frac{4\pi D_i M_i}{\rho_p RT}\left(\frac{3}{4\pi}\right)^{\frac{1}{3}}(p_i^\infty - p_i^{eq}). \tag{5}$$

The fraction $1/3$ is characteristic of diffusion processes and $\sigma_i(t)$ has the dimension of a diffusion coefficient μm^2 s^{-1}.

Let us give an idea of the value of $\sigma_i(t)$ in the case where species i is water: $D_i \simeq 10^{-4}$ m^2 s^{-1}, $M_i = 1.8 \times 10^{-2}$ kg mol^{-1}, $\rho_p = 10^3$ kg m^{-3}, $T = 300$ K, the water saturation vapor pressure for such temperature is approximately $p_i^{eq} \simeq 3000$ Pa.

In the case of condensation, we guess a vapor pressure $p_i^\infty = 2p_i^{eq}$, then σ_i is approximately equal to 1.7×10^4 μm^2 s^{-1} for pure water droplets.

Expression (4) of the condensation rate of i remains the same in the multicomponents case.

2.1.3. Nucleation kernel

Nucleation of vapor substances in the atmosphere can occur both homogeneously and heterogeneously, and may involve several chemical species as the well-known binary nucleation process H_2O–H_2SO_4.

Theoretical expressions for homogeneous nucleation can be obtained either from kinetic approach [20] or from thermodynamic considerations [3]. The nucleation rate can generally be written in the form

$$J_0(t) = C\exp\left(-\frac{\Delta G^*}{k_b T}\right), \tag{6}$$

where ΔG^* is the free energy required to form a stable nucleus and C is a constant depending mainly on vapor pressures of each chemical species. Some parameterizations of the nucleation rate are available in [21,22].

2.1.4. Deposition kernel

Aerosols can be removed from atmosphere either by deposing on any ground surfaces (dry deposition), or by sticking to rain drops (wet scavenging). The impact of both processes are usually proportional to the ASD, therefore the expression of aerosol loss by deposition is written in the form

$$\left(\frac{\partial n}{\partial t}\right)_{\text{dep}} = -R(v,t)n(v,t). \tag{7}$$

That is to note Eq. (7) describes a relaxation process where $1/R(v,t)$, time dimensioned, represents the life time in atmosphere of aerosols of size v.

In the case of dry deposition $R(v,t)$ is expressed in term of a deposition velocity $V_{\text{d}}(v,t)$ [18]

$$R(v,t) = \frac{V_{\text{d}}(v,t)}{\Delta z}, \quad V_{\text{d}}(v,t) = \frac{1}{R_{\text{a}} + R_{\text{b}} + R_{\text{a}}R_{\text{b}}V_{\text{s}}(v,t)} + V_{\text{s}}(v,t), \tag{8}$$

where Δz is the vertical reference height of the model, $V_{\text{s}}(v,t)$ the sedimentation velocity of aerosols of size v, R_{a} the aerodynamic resistance between the reference height and the ground, and R_{b} is the resistance to Brownian diffusion in the laminar sublayer just above the surface. The expression of V_{d} is obtained by analogy with electric circuits.

2.2. Principles and mass flow equation

The coagulation process is quite difficult to modelize in terms of stochastic dynamics because of its non-linearity. Let us first briefly summarize the stochastic methods already developed for coagulation.

As the coagulation term is non-linear in the ASD $\tilde{q}$ (10), it would then be necessary to know the density $\tilde{q}$ to simulate exactly the coagulation process. But the density $\tilde{q}$ is precisely the quantity we want to compute.

The key idea to overcome this difficulty is that according to the law of large numbers, the density may be approximated by the empirical measure of a large number of particles. This leads to work with a large number of numerical particles and to replace $\tilde{q}$ by the empirical measure in the coagulation mechanism. In fact non-linearity is replaced by interactions between particles. As a consequence coagulation is treated accurately only if the number of numerical particles, let us note P, is large enough to ensure that the mean-field asymptotics holds.

Stochastic algorithms for coagulation mainly differ whether what is associated with one numerical particle.

To fix one's mind let us consider one numerical particle labeled by i. In [17] Lushnikov associates with this particle one physical aerosol of size y_i. The drawback of this method is that the number of particles decreases as coagulation makes the number of aerosol decrease, which is a strong limitation as coagulation converges in the limit of the number of particles going to infinity.

To avoid this problem Babovsky in [1], Wagner and Eibeck in [2] associate with the particle one unit mass of aerosols of size $y_i(t)$ at time t. Then the particle represents a number $1/y_i(t)$ of aerosols of size y_i at time t. As coagulation physically preserves the total aerosol mass, the number P of numerical particles remains constant. This kind of algorithm is then called "mass flow algorithm," let us note MFA.

The next step is to extend the MFA to condensation/evaporation, nucleation, and removal. The total aerosol mass being now likely to vary, a first idea is to allow the number P of particle to vary along time

[23], as this one is directly linked to the total aerosol mass in MFA. But P decreases with evaporation and removal, which we would like to avoid for the same previous reasons.

In order to keep a particle number at least non-decreasing, a second idea is to allow the unit mass of aerosols of each numerical particle to vary, let us note $\omega_i(t)$ this varying mass for the ith particle at time t, in the previous MFA $\omega_i(t)$ was always equal to unity. The ith particle now stands for a number $(\omega_i/y_i)(t)$ of physical aerosols of size $y_i(t)$. The varying mass $\omega_i(t)$ is connected to the condensation/evaporation and removal processes, which no longer affect the number of numerical particles.

As the nucleation process is independent of already existing aerosols, it cannot be related to preexisting numerical particles, and has to be treated by creation of new numerical particles. Then P may increase by nucleation, which has no impact on the algorithm convergence.

The MFA is based on the aerosol relative mass density $\tilde{q}(v,t)$

$$\tilde{q}(v,t) = \frac{q(v,t)}{Q_0}, \quad Q_0 = \int_{v_0}^{\infty} q_0(v)\,\mathrm{d}v. \tag{9}$$

From (1) one easily gets (calculations are reported in Appendix B)

$$\begin{aligned}\frac{\partial \tilde{q}}{\partial t}(v,t) = &\underbrace{\int_{v_0}^{v-v_0} Q_0 \frac{K(u,v-u)}{v-u}\tilde{q}(u,t)\tilde{q}(v-u,t)\,\mathrm{d}u - \tilde{q}(v,t)\int_{v_0}^{\infty} Q_0 \frac{K(v,u)}{u}\tilde{q}(u,t)\,\mathrm{d}u}_{\text{non linear terms of coagulation}} \\ &+ \underbrace{\left(\frac{I_0(v,t)}{v} - R(v,t)\right)\tilde{q}(v,t)}_{\text{non conservative terms}} - \underbrace{\frac{\partial(I_0\tilde{q})}{\partial v}(v,t)}_{\text{conservative term}} + \underbrace{\frac{v_0 J_0(t)}{Q_0}\delta_{(v_0,v)}}_{\text{creation term}}.\end{aligned} \tag{10}$$

The three last terms on the right-hand side of (10) can be given an exact probabilistic interpretation at the continuous time level. Let us underline that some kernels have been modified. The relevant kernels are now $Q_0(K(u,v)/v)$ for coagulation, $I_0(v,t)/v$ for condensation/evaporation, and $v_0 J_0(t)/Q_0$ for nucleation.

3. Mass flow algorithm

The common idea of stochastic algorithms is to make a large number of independent experiments (let us say MC) and to average over them. This is called the Monte-Carlo loop.

The state of the system within each experiment is represented at time t by the array of numerical particles $[(y_i^t, \omega_i^t),\ i = 1,\ldots,P^t]$, where P^t is the number of numerical particles at time t.

The relative densities are approximated by the sum of Dirac[3] masses

$$\tilde{n}(v,t) = \frac{1}{P^0}\sum_{i=1}^{P^t}\omega_i(t)\delta_{(y_i(t),v)}, \quad \tilde{q}(v,t) = \frac{1}{P^0}\sum_{i=1}^{P^t}\omega_i(t)\delta_{(y_i(t),v)}. \tag{11}$$

Note that both relative densities are divided by the initial number of particles P_0.

The aerosol size spectrum $[v_0, v_{\max}]$ is discretized in a finite number NB of regular bins $1 \leqslant l \leqslant NB$, $B_l = [v_l^-, v_l^+]$, $v_l^+ - v_l^- = \Delta v$, then the densities (11) are approximated by piecewise constant functions

$$v \in B_l, \qquad \tilde{n}(v,t) = \frac{1}{P^0}\sum_{i=1}^{P^t}\omega_i^t\delta_{(y_i^t \in B_l)}, \quad \tilde{q}(v,t) = \frac{1}{P^0}\sum_{i=1}^{P^t}\frac{\omega_i^t}{y_i^t}\delta_{(y_i^t \in B_l)}. \tag{12}$$

[3] δ is the Kronecker symbol.

The choice of $v_{\max}$ does not modify the algorithm, it depends only on the aerosol size spectrum that one wants to focus on.

In order to make the average over the *MC* experiments, one needs to conserve the aerosol concentration and mass in each bin l, which we, respectively, call N_l and Q_l. These two arrays are set to zero before the Monte-Carlo loop but are not reinitialized during the Monte-Carlo loop, on the contrary to (y_i, ω_i).

3.1. Description

The extended MFA is then the following over a time period $[0, T]$:

Algorithm 1 (*Extended MFA*).

$[(N_l, Q_l) = (0, 0),\ i = 1, \ldots, P^0]$

1. Monte-Carlo loop $(1 \leqslant mc \leqslant MC)$

a. Initialization: Calculation of $[(y_i^0, \omega_i^0),\ i = 1, \ldots, P^0]$

b. Time loop: $[0, T]$

i. Calculation of a time step τ_k

ii. Integration of (10) **from** t_k **to** $t_{k+1} = t_k + \tau_k$:

Integration of coagulation:

$$\left(y_i^k, \omega_i^k\right) \to \left(y_i^{k+\frac{1}{2}}, \omega_i^{k+\frac{1}{2}}\right)$$

Integration of condensation/evaporation and deposition:

$$\left(y_i^{k+\frac{1}{2}}, \omega_i^{k+\frac{1}{2}}\right) \to \left(y_i^{k+1}, \omega_i^{k+1}\right)$$

Integration of nucleation:

creation of J new particles

iii. Removal of numerical particles:

if $y_i^{k+1} \leqslant v_0$ then the i^{th} particle is removed.

c. Updating of concentration and mass densities:

From $i = 1, \ldots, P^T$ if $y_i^T \in B_l$

then $Q_l \leftarrow Q_l + \omega_i^T$ and $N_l \leftarrow N_l + \omega_i^T / y_i^T$

2. Averaging on the MC experiments.

At the end of the Monte-Carlo loop, N_l and Q_l are averaged over the *MC* experiments: $N_l \leftarrow N_l \times Q_0/MC/P^0$ and $Q_l \leftarrow Q_l \times Q_0/MC/P^0$

The Mass Flow Algorithm is related to the appropriate choice of the sequence of discrete times (t_k). The time step $\tau_k = t_{k+1} - t_k$ is computed on the basis of the kernels. The new state at time t_{k+1} is computed by taking into account in a sequential way coagulation, condensation/evaporation, deposition, and nucleation. The order of the sequence has no impact on the algorithm's convergence.

We now give some details for each step.

3.2. Initialization

This step consists in calculating the initial state $[(y_i^0, \omega_i^0),\ i = 1, \ldots, P^0]$ according to a given mass density $v \mapsto q_0(v)$.

The mass ω_i of each particle i is set to unity $\forall i = 1, \ldots, P^0$, $\omega_i^0 = 1$. The calculation of $[y_i^0,\ i = 1, \ldots, P^0]$ may be performed:

- either by randomly generating each y_i^0, independently according to the probability density, $v \mapsto \tilde{q}_0(v)$;
- or by using a deterministic initialization based on the associated cumulative distribution function:

$$y_i^0 = \inf\left(v \Big/ \int_{v_0}^{v} \tilde{q}_0(u)\,\mathrm{d}u \geqslant \frac{2i-1}{2P^0}\right). \tag{13}$$

3.3. Time step

Choosing the appropriate time step is a key issue. On the one hand the time step is supposed to be small enough compared to time scales of physical processes in order to allow an accurate integration. On the other hand it is expected to be large enough to avoid a prohibitive CPU time.

Let us then define the time scale of each physical process.

- For coagulation between aerosols of size y_i^k and y_j^k:

$$\frac{y_j^k}{Q_0 \omega_j^k K(y_i^k, y_j^k)}. \tag{14}$$

- For condensation/evaporation of aerosols of size y_j^k:

$$\frac{y_j^k}{|I_0(y_j^k, t_k)|}. \tag{15}$$

- For deposition of aerosol of size y_j^k:

$$\frac{1}{R(y_j^k, t_k)}. \tag{16}$$

- For nucleation of aerosols:

$$\frac{Q_0}{v_0 J_0(t)}. \tag{17}$$

As the coagulation kernel is unbounded the smallest time scale is usually due to coagulation. Let us note $1/\lambda_k$ the smallest time scale for coagulation whose expression is derived from (14)

$$\lambda_k = Q_0 \max_{i,j=1,\ldots,P^k} \left(\frac{\omega_j^k K(y_i^k, y_j^k)}{y_j^k}\right). \tag{18}$$

Then τ_k is usually defined as [1]

$$\tau_k = \frac{c}{\lambda_k}, \tag{19}$$

where c is a constant, As c^2 is the proportion of particles which should coagulate twice, c must be kept small, it is usually equal to 0.1.

In practice, to ensure an accurate integration of other processes one has to check that τ_k remains small compared to (15)–(17).

The calculation of λ_k (18) requires a double loop on P^k, which can be expensive in CPU time if P^k becomes large. For most coagulation kernels this double loop can be avoided, we give further details in Appendix C.

3.4. Calculation of the state at t_{k+1}

The calculation of the new state of the system at time t_{k+1} is performed by the successive integration of each physical process, the order of integration has no impact on the numerical solution and the algorithm's convergence.

3.4.1. Integration of coagulation

An array of integers J_i, $i = 1, \ldots, P^k$, and an array of real numbers U_i, $i = 1, \ldots, P^k$, are randomly generated with the respective uniform probability laws over $[1, \ldots, P^k]$ and $[0, 1]$.

Integration of coagulation is performed by making coagulate the numerical particle i ($i = 1$ to P^k) and J_i if the following condition is met:

$$i = 1, \ldots, P^k, \qquad y_i^{k+\frac{1}{2}} \leftarrow y_i^k + y_{J_i}^k \quad \text{if } U_i \leqslant \underbrace{Q_0 \frac{K(y_i^k, y_{J_i}^k)}{y_{J_i}^k} \omega_{J_i}^k \tau_k}_{A}. \tag{20}$$

The calculation of τ_k ensures that A always within $[0, 1]$.

3.4.2. Integration of condensation/evaporation and deposition

This step is performed in a deterministic way, that is to say through the integration over the time step τ_k of the following ODE system:

$$i = 1, \ldots, P^k, \qquad \dot{y}_i = I_0(y_i, t), \quad \dot{\omega}_i = \omega_i \left(\frac{I_0(y_i, t)}{y_i} - R(y_i, t) \right) \tag{21}$$

with $(y_i^{k+\frac{1}{2}}, \omega_i^{k+\frac{1}{2}})$ as initial values. Provided the time step τ_k is small compared to the time scales of condensation/evaporation and deposition, Eq. (21) can be solved by an explicit Euler scheme:

$$i = 1, \ldots, P^k, \qquad y_i^{k+1} = y_i^{k+\frac{1}{2}} + \tau_k I_0\left(y_i^{k+\frac{1}{2}}, t_k\right), \quad \omega_i^{k+1} = \omega_i^{k+\frac{1}{2}} \frac{y_i^{k+1}}{y_i^{k+\frac{1}{2}}} \mathrm{e}^{-\tau_k R\left(y_i^{k+\frac{1}{2}}, t_k\right)}. \tag{22}$$

Letting the weights ω_i of particles evolve with condensation/evaporation and deposition enables to keep the number of particles constant.

3.4.3. Integration of nucleation

According to Eq. (10) the nucleation process produces a global mass $v_0 J_0(t_k)\tau_k$ of aerosols of size v_0 within the time step τ_k.

This mass is created independently from already existing aerosols on the contrary to condensation/evaporation, new numerical particles have then to be created to represent this incoming mass.

Then we define J new numerical particles

$$\omega_i = 1, \quad y_i^{k+1} = v_0, \quad i = P^k + 1, \ldots, P^k + J, \tag{23}$$

where J is the integral part of $v_0 J_0(t_k)\tau_k$. The fractionary part of $v_0 J_0(t_k)\tau_k$ can be treated

- either by creating a new numerical particle with weight $\omega_{P^k+J+1} = 1$ if the following condition is met:

$$U \leqslant v_0 J_0(t_k)\tau_k - J, \tag{24}$$

where U is a real number randomly generated with the uniform probability law over $[0, 1]$

- or by creating a new numerical particle with modified weight

$$\omega_{P^k+J+1} = v_0 J_0(t_k)\tau_k - J. \tag{25}$$

The number of numerical particles is then increased, $P^{k+1} = P^k + J$ or $P^{k+1} = P^k + J + 1$.

4. Some numerical tests

4.1. Numerical setup

Analytical solutions of the GDE (1) are available for academic cases only, i.e., constant or linear kernels, and assuming $v_0 = 0$. In the case of coupled coagulation and condensation, academic cases are nevertheless interesting as they represent the limiting behavior of an ASD undergoing such processes.

Some analytical solutions are available with the following initial densities and kernels [24]:

- Initial ASD:

$$\text{(a) } n_0(v) = \frac{n_0}{v_\mathrm{m}} \exp\left(-\frac{v}{v_\mathrm{m}}\right), \tag{26}$$

  where v_m and n_0 are, respectively, the mean aerosol volume and the total aerosol concentration. We choose $v_\mathrm{m} = 0.029\ \mu\mathrm{m}^3$ and $n_0 = 10^6 \#\text{aerosols}\ \ \mathrm{cm}^{-3}$.
- (1) Constant coagulation and constant condensation:

$$K(u,v) = K_0, \quad I(v,t) = \sigma. \tag{27}$$

- (2) Constant coagulation and linear condensation:

$$K(u,v) = K_0, \quad I(v,t) = \sigma v. \tag{28}$$

- (3) Linear coagulation and linear condensation:

$$K(u,v) = K_0(u+v), \quad I(v,t) = \sigma v, \tag{29}$$

  where K_0 and σ are constants.

In Table 1, for each case we define the time scales of coagulation (τ_c) and condensation (τ_d), the ratio between characteristic times (Λ), and the dimensionless total number ($M_0(t)$) and mass concentration ($M_1(t)$).

One can check that the time scale of coagulation is the time period at the end of which the total aerosol concentration is divided by two for (1) and (2), by $\mathrm{e}^{1-e} \simeq 0.18$ for (3) assuming Λ close to unity.

In the same way the time scale of condensation is the time period at the end of which the total aerosol volume is multiplicated by $1 + \ln(2) \simeq 1.7$ for (1) assuming Λ close to unity, by e for (2) and (3).

Moments in case (2) are not coupled, i.e., M_0 depend only of coagulation and M_1 only of condensation. That is why cases (1) and (3) are also interesting as M_1 in case (1) and M_0 in case (3) depend of both physical processes.

Table 1
Time scales and dimensionless moments

	τ_c	τ_d	$\Lambda = \tau_\mathrm{c}/\tau_\mathrm{d}$	$M_0(t)$	$M_1(t)$
(1)	$2/K_0 n_0$	v_m/σ	$2\sigma/K_0 n_0 v_\mathrm{m}$	$1/(1+\frac{t}{\tau_\mathrm{c}})$	$1 + \Lambda \ln(1+\frac{t}{\tau_\mathrm{c}})$
(2)	$2/K_0 n_0$	$1/\sigma$	$2\sigma/K_0 n_0$	$1/(1+\frac{t}{\tau_\mathrm{c}})$	$\exp(\frac{t}{\tau_\mathrm{d}})$
(3)	$1/K_0 n_0 v_\mathrm{m}$	$1/\sigma$	$\sigma/K_0 n_0 v_\mathrm{m}$	$\exp\frac{1}{\Lambda}\left(1-\exp\left(\frac{t}{\tau_\mathrm{d}}\right)\right)$	$\exp(\frac{t}{\tau_\mathrm{d}})$

We give the solution $v \mapsto n(v,t)$ for each case, they are obtained by Laplace transform [24] with the initial density (a), the ASD moments M_0 and M_1 are derived in Table 1.

- (1) Constant coagulation and constant condensation:

$$n(v,t) = \frac{n_0}{v_m} \frac{(M_0)^2}{M_1 + \Lambda(M_0 - 1)} \exp\left(- \frac{\frac{v}{v_m} M_0 + \Lambda(M_0 - 1)}{M_1 + \Lambda(M_0 - 1)} \right) \tag{30}$$

this is an approximation of the analytical solution, valid for $v \geqslant v_m \Lambda(1 + (t/\tau_c))$.

- (2) Constant coagulation and linear condensation:

$$n(v,t) = \frac{n_0}{v_m} \frac{(M_0)^2}{M_1} \exp\left(- \frac{v}{v_m} \frac{M_0}{M_1} \right). \tag{31}$$

- (3) Linear coagulation and linear condensation:

$$n(v,t) = n_0 \frac{M_0}{v\sqrt{1 - M_0}} \exp\left(- (1 - M_1)(2 - M_0) \frac{v}{v_m} \right) I_1\left(2(1 - M_1)\sqrt{1 - M_0} \frac{v}{v_m} \right), \tag{32}$$

where I_1 is the modified Bessel function of first kind and first order.

If $\Lambda \ll 1$ the characteristic time of coagulation is much shorter than this of condensation, which means that, within a time period τ_c, condensation may be neglected as compared to coagulation. On the contrary if $\Lambda \gg 1$ condensation dominates the ASD evolution. In order to have a real coupling between both processes we then choose Λ equal to 1.

In case (1) the coagulation constant is chosen as the Brownian constant (3), in case (2) and (3) the coagulation and condensation constants are chosen so that time scales are equal to those of case (1). Numerical values of kernels and time scales are gathered in Table 2.

4.2. Calculations of errors

We compute the mean relative quadratic error for the concentration density:

$$\text{error} = \sqrt{\int_0^\infty \left(\frac{n^{\text{num}}(v,T) - n^{\text{th}}(v,T)}{n^{\text{th}}(v,T)} \right)^2 \mathrm{d}v}, \tag{33}$$

where $v \mapsto n^{\text{num}}(v,T)$ is the mean numerical density over the MC experiments and $v \mapsto n^{\text{th}}(v,T)$ is the theoretical density.

As the aerosol size spectrum is discretized in NB bins of width Δv, the integral in Eq. (33) is approximated by

$$\Delta v \sum_{l=1}^{NB} \left(\frac{n^{\text{num}}(v_l,T) - n^{\text{th}}(v_l,T)}{n^{\text{th}}(v_l,T)} \right)^2, \tag{34}$$

where $v_l = (v_l^+ - v_l^-)/2$.

Table 2
Numerical values for kernels and time scales

	K_0	σ	τ_c	τ_d	Λ
(1)	6.405×10^{-10} cm^3 s^{-1}	9.2×10^{-6} μm^3 s^{-1}	∼3122.6 s	∼3122.6 s	∼1
(2)	6.405×10^{-10} cm^3 s^{-1}	3.202×10^{-4} s^{-1}	∼3122.6 s	∼3122.6 s	∼1
(3)	1.115×10^{-8} cm^3 μm^{-3} s^{-1}	3.202×10^{-4} s^{-1}	∼3122.6 s	∼3122.6 s	∼1

4.3. Tests

4.3.1. Convergence characterization

We have tested the convergence of the algorithm in the case (2) after a time period $\tau_c/2$. The final volume density is shown in Fig. 8.

The main parameters of the MFA algorithm are the number of numerical particles, P, and the number of Monte-Carlo experiments, MC.

Fig. 1 illustrates the decrease of quadratic errors with respect to P and Fig. 2 with respect to MC.

The asymptotic behavior of the relative quadratic error turns out to be one expected with stochastic algorithms:

$$\text{error} \sim \frac{1}{\sqrt{MC \times P}} \tag{35}$$

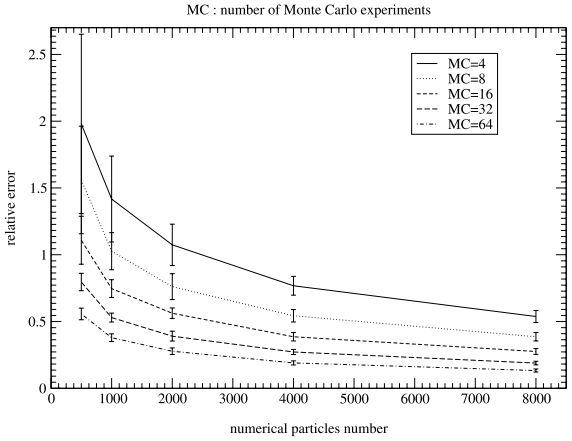

Fig. 1. Relative quadratic error on the concentration density in function of the numerical particles number.

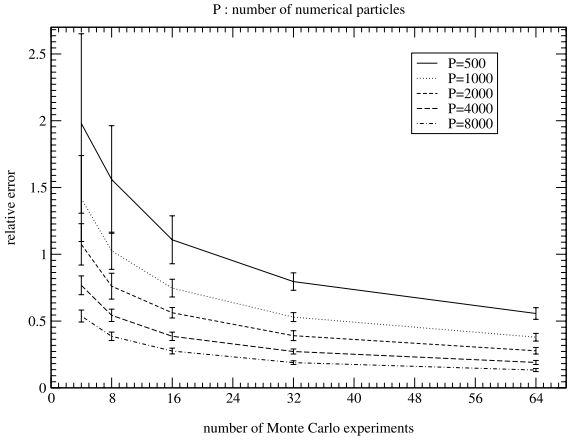

Fig. 2. Relative quadratic error on the concentration density in function of the Monte-Carlo number.

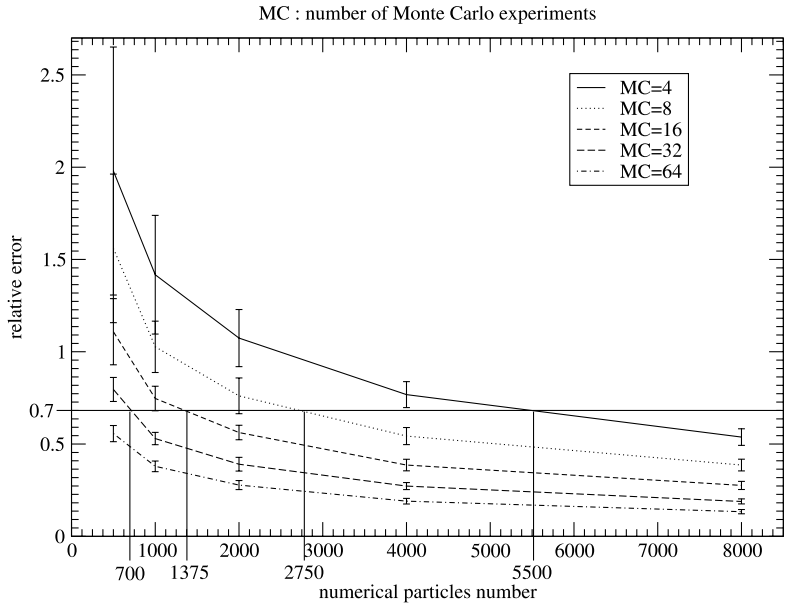

Fig. 3. Relative quadratic error the concentration density, illustration of the accuracy funtion of $MC \times P$.

which suggests the existence of a "central limit theorem" for coupled coagulation condensation. We must point out that Eq. (35) represents an asymptotic result, indeed to make MC run to infinity, keeping P constant, will not allow the error to vanish, because the convergence of coagulation, a non-linear process, is achieved with P going to infinity. Eq. (35) implies that accuracy is asymptotically proportional to the product $MC \times P$. Indeed we check in Fig. 3 that for a given accuracy, let us say 0.7, the product $MC \times P$ remains roughly constant equal to 22,000.

As stochastic methods are usually expensive in terms of calculation time, it is also interesting to determine the CPU time behavior with respect to MC and P. Figs. 4 and 5 show, respectively, in LOG10 scale the CPU time in function of P and MC. It is found that the CPU time evolves as

$$\text{CPU} \sim MC \times P\sqrt{P}. \tag{36}$$

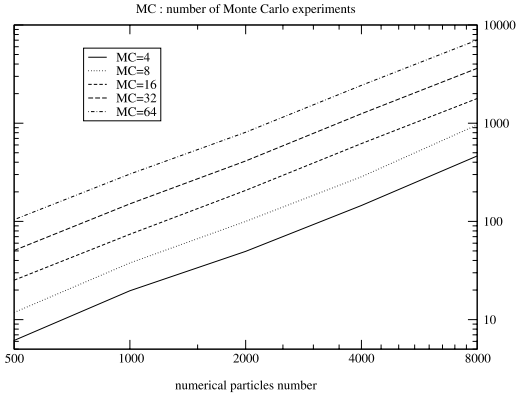

Fig. 4. CPU time in function of the numerical particle number, LOG10 scale.

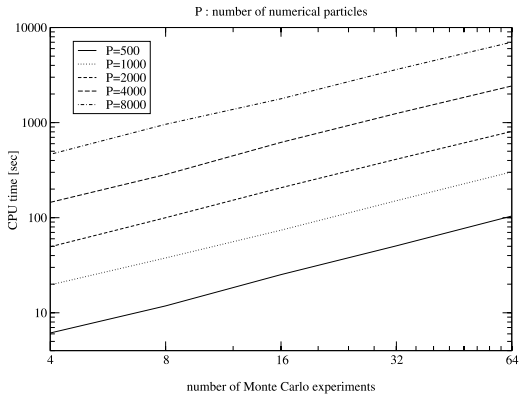

Fig. 5. CPU time in function of the Monte-Carlo number, LOG10 scale.

As we would like a good accuracy with a CPU time as low as possible, we investigate the ratio between accuracy and CPU time:

$$\text{accuracy} \sim MC \times P \Rightarrow \frac{\text{accuracy}}{\text{CPU}} \sim \sqrt{P}. \tag{37}$$

As we have pointed out with Eq. (35), Eq. (37) represents an asymptotic behavior, then provided P is large enough, it suggests that for a given accuracy one has better to take a number of numerical particles as low as possible with appropriate cycling.

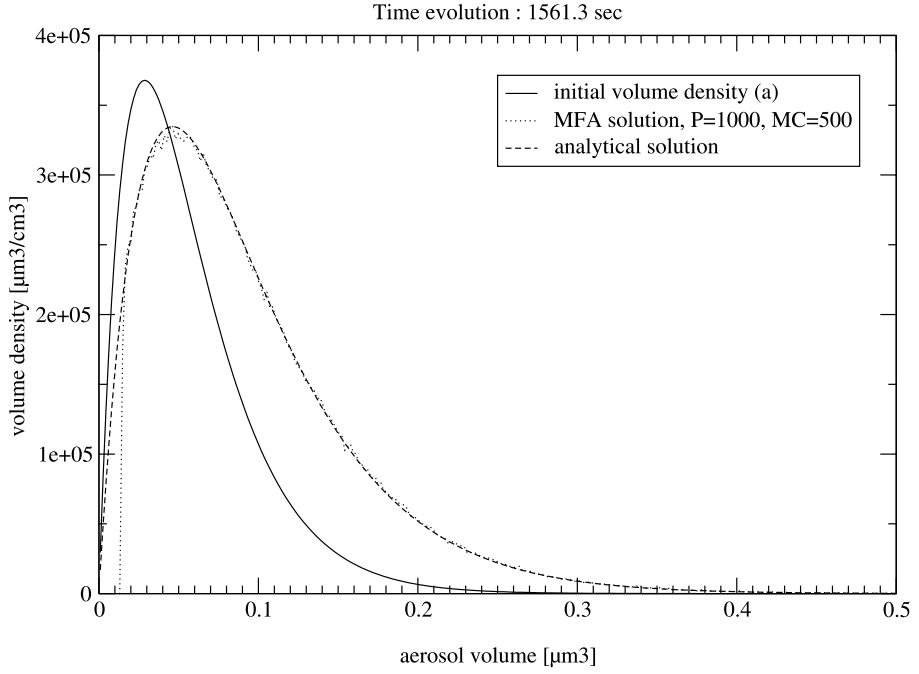

Fig. 6. Constant coagulation and constant condensation, CPU time = 106 s.

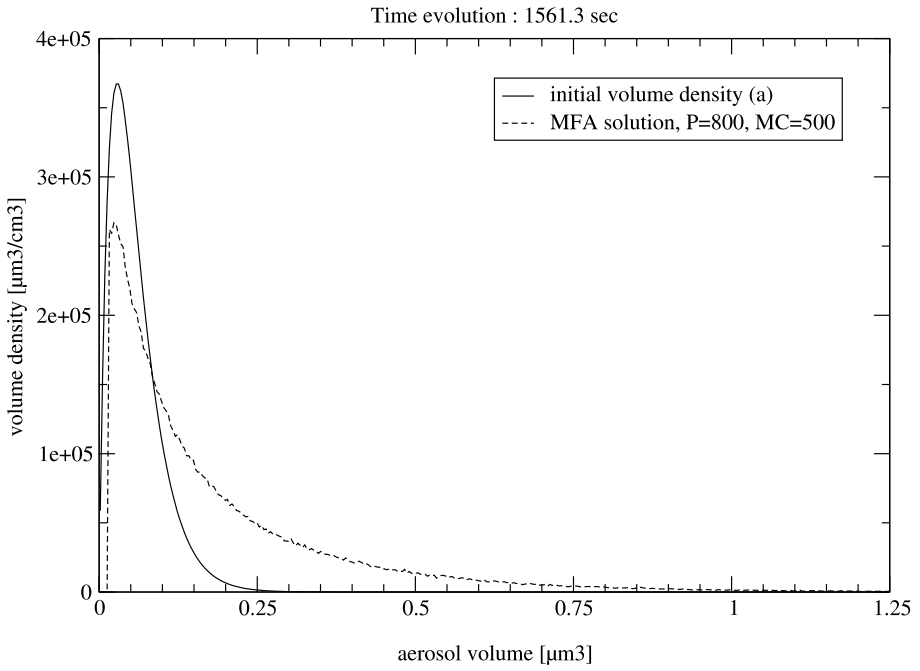

Fig. 7. Linear coagulation and constant condensation, CPU time = 1053 s.

The results obtained here does not depend on the exact solution taken, therefore we do not repeat these results for all cases.

4.3.2. Limiting cases

For atmospheric aerosols the coagulation and condensation/evaporation are generally bounded as follows:

$$K(u,v) \leqslant C(u+v), \quad I_0(v,t) \leqslant \sigma v. \tag{38}$$

Constant and linear kernels appear to be limiting cases for both processes, therefore it appears interesting to investigate the algorithm's behavior for such cases. Furthermore linear coagulation appears for turbulent diffusion and linear condensation is encountered when chemical reactions occur near the aerosol surface.

Figs. 8 and 9 with linear condensation are characterized by an accumulation of particles at large sizes. Small particles are never completely removed since the condensation rate vanishes for small particles. Linear coagulation emphasizes this spreading effect towards large sizes compared to constant coagulation.

That is to note that as the linear coagulation also vanishes for small volumes, small aerosols are removed neither by condensation nor coagulation, which results in a ASD pick on small aerosols.

Cases with constant condensation (Figs. 6 and 7) are characterized by the fact that at any time t there remain no aerosols smaller than σt, i.e., $v_m(t/\tau_c)$. Then after the time period $\tau_c/2$ the ASD breaks down below 0.014 μm^3.

As the condensation does not spread the ASD all over the size spectrum, the maximum of the volume density decreases slowerly then linear condensation.

That is to note the approximation of the analytical solution in case (1) (Fig. 6) is not reliable below $1.5v_m$, i.e., 0.043 μm^3.

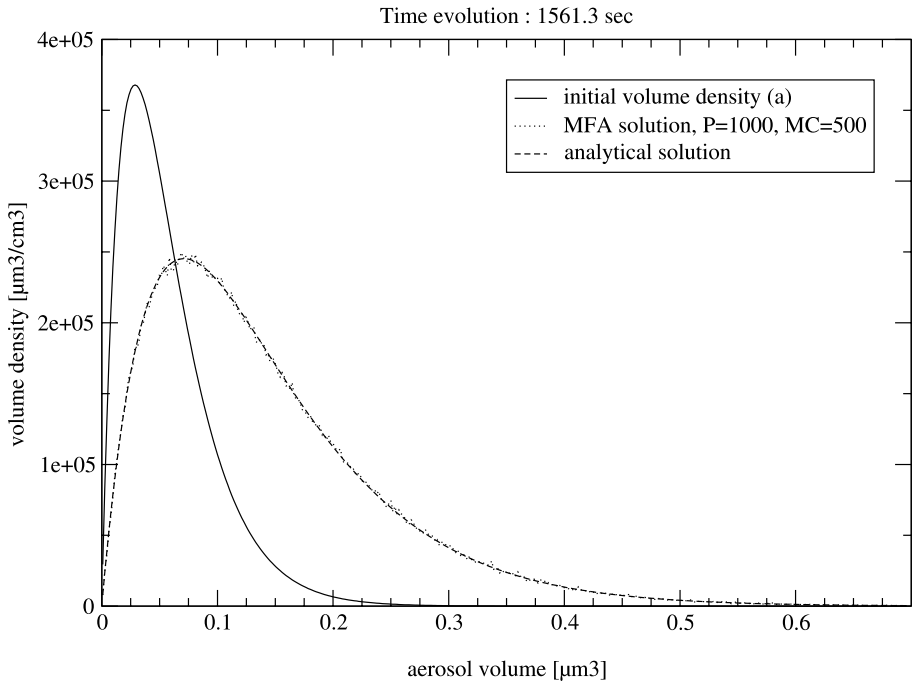

Fig. 8. Constant coagulation and linear condensation, CPU time = 107 s, relative error = 0.55.

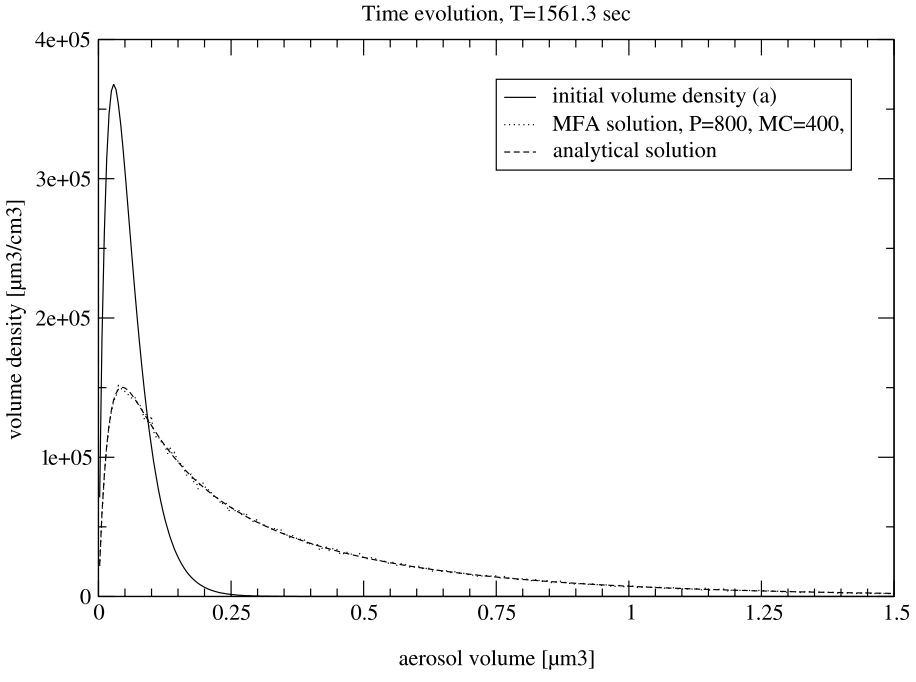

Fig. 9. Linear coagulation and linear condensation, CPU time = 878 s, relative error = 0.28.

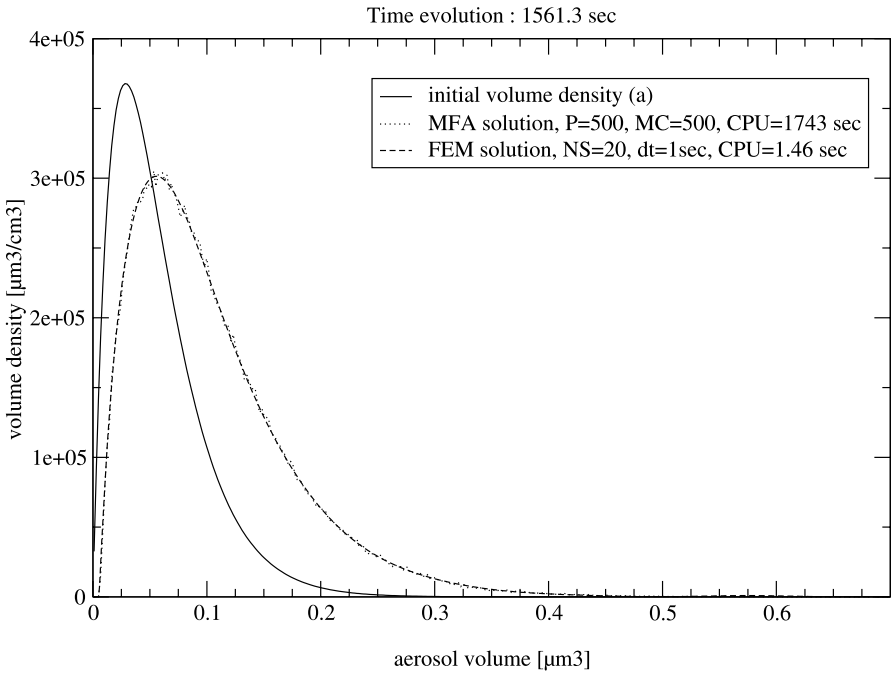

Fig. 10. Brownian coagulation and diffusive condensation.

4.3.3. Realistic cases

We present in Fig. 10, a comparison between the MFA and a finite element method, let us note FEM, in the case of Brownian coagulation and diffusive condensation limited to the continuous regime, for which kernels are defined in Sections 2.1.1 and 2.1.2. In this case the GDE admits no analytical solution.

Finite element or collocation methods have already been developed, we refer here to [11,12,25]. They differ depending on the kind of finite elements used. The one we have been developing is based on a spectral decomposition on orthogonal polynomials. The FEM enables to solve the GDE in a coupled way and seems to be reliable for operational 3D models.

Time scales of coagulation and condensation depend on the aerosol size, nevertheless one can define average time scales for both processes

$$\tau_c = \frac{2}{K_0 n_0}, \quad \tau_d = \frac{(v_m)^{\frac{2}{3}}}{\sigma}. \tag{39}$$

We choose K_0 as the Brownian constant (3) and in order to have comparable time scales we determine σ so that $\tau_c = \tau_d$, then $\sigma = 3 \times 10^{-5}$ µm^2 s^{-1}, although it may not be a realistic time scale for condensation.

5. Conclusion

- We have presented in this article a new algorithm based on a stochastic mass flow formulation for the integration of the GDE of monocomponent aerosols. The key point is that this algorithm may serve as a reference solution for benchmarking other numerical methods intended for insertion in three dimension

models. On the contrary to many other algorithms, the theoretical basis is well found, which ensures convergence results. This algorithm is moreover easy to implement.
- This algorithm can be quite easily extended to multicomponents aerosols, the mass $\omega_i(t)$ of the ith particle is then split into $s = 1, \ldots, c, \omega_i^s(t)$, where c is the number of chemical species involved. By getting the mass flow equation for the multicomponent case, one can adjust the integration of each process.
- Future works concern the search for algorithms to be used in a 3D framework. The first step will be the validation of such methods by comparison with the mass flow algorithm.

Acknowledgements

We thank our colleagues Gilles Bergametti (LISA), Bernard Aumont (LISA), and Luc Musson-Genon (EDF-CEREVE) for fruitful discussions. This work is a part of a common project devoted to aerosol modeling.

Appendix A. Full expressions of kernels

A.1. Coagulation kernel

- In the continuous regime:

$$K_c(u,v) = 4\pi(D_u + D_v)(r_u + r_v), r_u = \left(\frac{3u}{4\pi}\right)^{\frac{1}{3}}, \tag{A.1}$$

where r_u and D_u are, respectively, the aerosols radius and the diffusion coefficient for aerosols of size u, this latter can be easily estimated in the continuous regime from Einstein relation

$$D_u = \frac{k_b T}{6\pi\mu_{air} r_u}, \tag{A.2}$$

where k_b is Boltzmann's constant, T the temperature, and μ_{air} is the dynamic viscosity of air.
- In the free molecular regime:

$$K_m(u,v) = \pi(r_u + r_v)^2(c_u^2 + c_v^2)^{\frac{1}{2}}, \quad c_u = \left(\frac{8k_b T}{\pi\rho_p u}\right)^{\frac{1}{2}} \tag{A.3}$$

where ρ_p is the specific mass of aerosols, assumed to be independent of the aerosol size, and c_u is the mean speed of aerosols of size u, derived from the Kinetics theory of gases.

Between both regimes, i.e., $0.1 \leqslant K_n \leqslant 10$, Eqs. (A.1) and (A.3) may not be valid. A theoretical correcting function f was proposed by Fuchs [26] for the transition regime, using the limit sphere method

$$K(u,v) = K_c(u,v) f(u,v), \quad f(u,v) = \left(\frac{r_u + r_v}{r_u + r_v + g_{uv}} + \frac{4(D_u + D_v)}{(c_u^2 + c_v^2)^{\frac{1}{2}}(r_u + r_v)}\right)^{-1} \tag{A.4}$$

with

$$g_{uv} = (g_u^2 + g_v^2)^{\frac{1}{2}}, \quad g_u = \frac{1}{6 r_u \lambda_u}\left[(2r_u + \lambda_u)^3 - (4r_u^2 + \lambda_u^2)^{3/2}\right] - 2r_u, \quad \lambda_u = \frac{8D_u}{\pi c_u}. \tag{A.5}$$

From the continuous to the transition regime, the diffusion coefficient D_u has also to be corrected as follows:

$$D_u = \frac{k_b T}{6\pi\mu_{air} r_u} C_{un}, \tag{A.6}$$

where C_{un} is a correction factor, usually called Cunningham coefficient. Several expressions of C_{un} have been proposed, either empirically [27] or theoretically [28]. A now widely used expression is the one of Phillips [29] who obtains by solving Boltzmann's equations around a spherical particle

$$C_{un} = \frac{5 + 4c_1 K_n + 3(c_1^2 + 1)K_n^2 + 6c_2(c_1^2 + 2)K_n^3}{5 - c_1 K_n + c_2[(8 + \pi\alpha)/3](c_1^2 + 2)K_n^2} \tag{A.7}$$

with $c_1 = (2 - \alpha)/\alpha$, $c_2 = 1/(2 - \alpha)$, and α a slipping coefficient, giving the probability that molecules slip to the particle's surface.

A.2. Condensation/evaporation kernel

The condensation/evaporation kernel in the free molecular regime is given by

$$I_0^m(v,t) = \pi(r_v)^2 \alpha c_i \frac{M_i}{RT}(p_i^\infty - p_i^{eq}), \quad r_v = \left(\frac{3v}{4\pi}\right)^{\frac{1}{3}}, \tag{A.8}$$

where M_i is the molar weight of species i, R the perfect gas constant, T the temperature, $p_i^\infty - p_i^{eq}$ the gradient of vapor pressure of i, α the probability for one gas molecule to stick to the aerosol, and c_i is the mean speed of molecules of species i, which is usually linked to the diffusion coefficient of i by $D_i = \lambda_{air} c_i/2$.

In the transition regime the condensation kernel can be interpolated by using the limit sphere method. The generalized kernel can be corrected from the continuous one (4) as follows:

$$I_0(v,t) = I_0^c(v,t) f(K_n, \alpha), \tag{A.9}$$

where $f(K_n, \alpha)$ is a correction function depending on the Knudsen number and α. Some theoretical expressions of f have been derived for spherical particles [28,30,31]. We give the widely employed expression of Dahneke [32]

$$f(K_n, \alpha) = \frac{1 + K_n}{1 + 2K_n(1 + K_n)/\alpha}, \quad K_n = \frac{r_v}{\lambda_{air}}. \tag{A.10}$$

One can check that for great Knudsen numbers Eq. (A.9) converges toward the theoretical expression in the free molecular regime (A.8).

Appendix B. Mass flow equation

The mass flow equation is the equation on the relative mass density. By multiplying (1) by the aerosol size v, one obtains

$$\frac{\partial q}{\partial t}(v,t) = \frac{v}{2}\int_{v_0}^{v-v_0} K(u, v-u)n(u,t)n(v-u,t)\,du - q(v,t)\int_{v_0}^{\infty} K(v,u)n(u,t)\,du - v\frac{\partial(I_0 n)}{\partial v}(v,t) + \delta_{(v_0,v)} v J_0(t). \tag{B.1}$$

The coagulation gain may be divided into two equal parts as $v = u + (v-u)$, then the fraction $1/2$ disappears, and the condensation term may be split by integration

$$v\frac{\partial(I_0 n)}{\partial v} = \frac{\partial(I_0 q)}{\partial v} - \frac{I_0 q}{v}, \tag{B.2}$$

we have then

$$\frac{\partial q}{\partial t}(v,t) = \int_{v_0}^{v-v_0} \frac{K(u,v-u)}{v-u} q(u,t)q(v-u,t)\,\mathrm{d}u - q(v,t)\int_{v_0}^{\infty} \frac{K(v,u)}{u} q(u,t)\,\mathrm{d}u - \frac{\partial(I_0 q)}{\partial v} + \frac{I_0 q}{v} + \delta_{(v_0,v)} v_0 J_0(t). \tag{B.3}$$

The mass flow equation is obtained by normalizing with the total initial aerosol mass Q_0

$$\frac{\partial \tilde{q}}{\partial t}(v,t) = \int_{v_0}^{v-v_0} Q_0 \frac{K(u,v-u)}{v-u} \tilde{q}(u,t)\tilde{q}(v-u,t)\,\mathrm{d}u - \tilde{q}(v,t)\int_{v_0}^{\infty} Q_0 \frac{K(u,v)}{u} q(u,t)\,\mathrm{d}u - \frac{\partial(I_0 \tilde{q})}{\partial v} + \frac{I_0 \tilde{q}}{v} + \frac{v_0 J_0(t)}{Q_0}\delta_{(v_0,v)}. \tag{B.4}$$

Appendix C. Calculation of λ_k

The definition of λ_k involves a double loop on the numerical particles due to the coagulation kernel

$$\lambda_k = Q_0 \max_{i,j=1,\ldots,P^k}\left(\frac{\omega_j^k K(y_i^k, y_j^k)}{y_j^k}\right). \tag{C.1}$$

This can be avoided by closely majorating λ_k, first we derive from (C.1)

$$\lambda_k \leqslant Q_0 \frac{\max_j \omega_j^k}{\min_j y_j^k} \times \max_{i,j} K(y_i^k, y_j^k). \tag{C.2}$$

As most coagulation kernels can be put in the form

$$K(u,v) = \frac{1}{2}(g(u)h(v) + h(u)g(v)) \tag{C.3}$$

the double loop is majorated by

$$\max_{i,j} K(y_i^k, y_j^k) \leqslant \max_i h(y_i^k) \times \max_j g(y_j^k). \tag{C.4}$$

Then by making four single loops we obtain an upper bound for λ_k

$$\lambda_k \leqslant Q_0 \frac{\max_j \omega_j^k}{\min_j y_j^k} \times \max_i h(y_i^k) \times \max_j g(y_j^k). \tag{C.5}$$

For example the continuous Brownian kernel (2) may be majorated as follows:

$$\max_{i,j} K(y_i^k, y_j^k) \leqslant \frac{2k_b T}{3\mu_{\mathrm{air}}}\left[2 + \max_{i,j}\left(\frac{y_i^k}{y_j^k}\right)^{\frac{1}{3}} + \max_{i,j}\left(\frac{y_j^k}{y_i^k}\right)^{\frac{1}{3}}\right] \leqslant \frac{4k_b T}{3\mu_{\mathrm{air}}}\left[1 + \left(\frac{\max_i(y_i^k)}{\min_i(y_i^k)}\right)^{\frac{1}{3}}\right]. \tag{C.6}$$

References

[1] H. Babovsky, On a Monte Carlo scheme for Smoluchowski's coagulation equation, Monte Carlo Methods and Applications 5 (1) (1999) 1–18.
[2] A. Eibeck, W. Wagner, Stochastic particle approximations for Smoluchowski's coagulation equation, Technical Report, Weierstrass-Institut for Applied Analysis and Stochastics, 2000. Preprint No. 585.
[3] J.H. Seinfeld, S.N. Pandis, Atmospheric Chemistry and Physics, Wiley–Interscience, New York, 1998.
[4] I.J. Ackermann, H. Hass, M. Memmesheimer, C. Ziegenbein, A. Ebel, The parameterization of the sulfate–nitrate–ammonia aerosol system in eurad, Meteorol. Atmos. Phys. 57 (1995) 101–114.
[5] Z. Meng, D. Dabdub, J.H. Seinfeld, Size-resolved and chemically resolved model of atmospheric aerosol dynamics, J. Geophys. Res. 103 (1998) 3419–3435.
[6] F.S. Binkowski, U. Shankar, The regional particulate matter model: model description and preliminary results, J. Geophys. Res. 100 (26) (1995) 191–209.
[7] E.R. Whitby, P.H. McMurry, Modal aerosol dynamics modeling, Aerosol Sci. Tech. 27 (1997) 673–688.
[8] M.Z. Jacobson, R.P. Turco, E.J. Jensen, O.B. Toon, Modeling coagulation among particles of different composition and size, Atmos. Environ. 28 (7) (1994) 1327–1338.
[9] J.M. Fernndez-Daz, C. Gonzlez-Pola Muiz, M.A. Rodrguez Braa, B. Arganza Garca, P.J. Garca Nieto, A modified semi-implicit method to obtain the evolution of an aerosol by coagulation, Atmos. Environ. 34 (2000) 4301–4314.
[10] S. Dhaniyala, A.S. Wexler, Numerical schemes to model condensation and evaporation of aerosols, Atmos. Environ. 30 (6) (1996) 919–928.
[11] A. Sandu, C.T. Borden, A framework for solving aerosol dynamics, Appl. Numer. Math., in print.
[12] C. Pilinis, Derivation and numerical solution of the species mass distribution equations for multicomponent particulate systems, Atmos. Environ. A 24 (7) (1990) 1923–1928.
[13] F. Gelbard, J.H. Seinfeld, Numerical solution of the dynamic equation for particulate systems, J. Comput. Phys. 28 (1977) 357–375.
[14] S. Tzivion, T.G. Reisin, Z. Levin, A numerical solution of the kinetic collection equation using high spectral grid resolution: a proposed reference, J. Comput. Phys. 148 (1999) 527–544.
[15] H. Babovsky, On a simulation scheme for the Boltzmann equation, Math. Method Appl. Sci. 8 (1986) 223–233.
[16] K. Nanbu, Stochastic solution method of the master equation and the model Boltzmann equation, Math. Method Appl. Sci. 8 (1986) 223–233.
[17] E.R. Domilovskii, A.A. Lushnikov, V.N. Piskunov, Monte Carlo simulation of coagulation processes, Dokl. Akad. Nauk SSSR Ser. Phys. Chem. 240 (1) (1978).
[18] M.Z. Jacobson, Fundamentals of Atmospheric Modeling, Cambridge University Press, Oxford, 1999.
[19] A. Nenes, S.N. Pandis, C. Pilinis, Isorropia: a new thermodynamic equilibrium model for multicomponent inorganic aerosols, Aquat. Geochem. 4 (1998) 123–152.
[20] J.L. Katz, M.D. Donohue, A kinetic approach to homogeneous nucleation theory, AIChE J. (1980) 137–153.
[21] A. Jaecker-Voirol, P. Mirabel, Heteromolecular nucleation in the sulfuric acid–water system, Atmos. Environ. 23 (1989) 2053–2057.
[22] J. Salles, J. Janischewski, A. Jaecker-Voirol, B. Martin, Mobile source emission inventory model. Application to Paris area, Atmos. Environ. 30 (12) (1996) 1965–1975.
[23] E. Debry, B. Jourdain, B. Sportisse, Modeling of aerosol dynamics: a stochastic algorithm, in: B. Sportisse (Ed.), Proceedings of APMS 2001, Geosciences, Springer, Berlin, 2001.
[24] T.E. Ramabhadran, T.W. Peterson, J.H. Seinfeld, Dynamics of aerosol coagulation and condensation, AIChE J. 22 (5) (1976) 840–851.
[25] C. Pilinis, J.H. Seinfeld, Mathematical modeling of the dynamics of multicomponent atmospheric aerosols, Atmos. Environ. 21 (4) (1987) 943–955.
[26] N.A. Fuchs, Mechanics of Aerosols, Pergamon Press, New York, 1964.
[27] R.A. Millikan, The general law of fall of a small spherical body through a gas, and its bearing upon the nature of molecular reflection from surfaces, Phys. Rev. 22 (1) (1923) 1–23.
[28] N.A. Fuchs, A.G. Sutugin, High Dispersed Aerosols, Pergamon Press, New york, 1971 (Topics in Current Aerosol Research (part 2)).
[29] W.F. Phillips, Drag on a small sphere moving through a gas, Phys. Fluids 18 (9) (1975) 1089–1093.
[30] S.K. Loyalka, Modeling of condensation on aerosols, Prog. Nucl. Energy 12 (1983) 1–8.
[31] M. Sitarski, Nowakowski, Condensation rate of trace vapor on Knudsen aerosols from solution of the Boltzmann equation, J. Colloid Interface Sci. 72 (1979) 113–122.
[32] B. Dahneke, Theory of Dispersed Multiphase Flow, Academic Press, New York, 1983.